Journal of Heat and Mass Transfer Research 8 (2021) 257 - 266

Journal of Heat and Mass Transfer Research

Journal homepage: http://jhmtr.semnan.ac.ir

Semnan University

Dufour and Soret Effect on Unsteady MHD Free Convection and Mass Transfer Flow Past an Impulsively Started Vertical Porous Plate Considering with Heat Generation

Meenakshi, V*,a

[a] *Osmania University, India.*

P A P E R I N F O

Paper history:
Received: 2020-09-06
Revised: 2021-08-11
Accepted: 2021-08-14

Keywords:
MHD;
Free-convection;
Unsteady flow;
Vertical plate;
Dufour and Soret effects
and Permeability.

A B S T R A C T

An analysis is carried out to study the effects of MHD, Dufour and Soret on unsteady free convection and mass transfer flow, past an impulsively started infinite vertical porous flat plate of a viscous incompressible and electrically conducting fluid in the presence of porous medium. The non-linear partial differential equations, governing the problem under consideration, have been transformed by a similarity transformation into a system of ordinary differential equations, which are linearized and then solved numerically by using the implicit finite difference method. The resulting velocity, temperature and concentration distributions are shown graphically for different values of the parameters entering into the problem. Finally, the numerical values of the local-skinfriction, local-Nusselt number, and local-Sherwood number are also presented in a tabular form.

DOI: 10.22075/JHMTR.2021.21229.1301

1. Introduction

The hydrodynamic flow of a viscous incompressible fluid past an impulsively started infinite horizontal plate was studied by Stokes [17], and because of its practical importance this problem was extended to bodies of different shapes by a number of researchers. Soundalgekar [16] studied the above problem along an infinite vertical plate, when it is cooled or heated by the free convection currents. It is also known that flows arising from differences in concentration have great significance not only for their own interest but also for the applications to geophysics, aeronautics and engineering. In light of the above applications, many researchers studied the effects of mass transfer on magneto hydrodynamics (MHD) free convection flow; some of them are, Raptis and Kafoussias [12], Rahman and Sattar [11], Yih [19], Aboeldahab and Elbarbary [1], Megahead et al. [9] and Kim [8]. In the above stated papers, the diffusion-thermo term and thermal-diffusion term were neglected from the energy and concentration equations respectively. But when heat and mass transfer occur simultaneously in a moving fluid, the relations between the fluxes and the driving potentials are of a more intricate nature. It has been found that an energy flux can be generated not only by temperature gradients but by composition gradients as well. The energy flux caused by a composition gradient is called Dufour or diffusion-thermo effect. On the other hand, mass fluxes can also be created by temperature gradients and this is the Soret or thermal-diffusion effect. In general, the thermal-diffusion and diffusion-thermo effects are of a smaller order of magnitude than the effects described by Fourier's or Fick's law and are often neglected in heat and mass transfer processes. However, exceptions are observed therein. The thermal-diffusion (Soret) effect, for instance has been utilized for isotope separation, and in mixtures between gases with very light molecular weight (H_2, He) and of medium molecular weight (N_2, air) the diffusion-thermo (Dufour) effect was found to be of a considerable magnitude such that it cannot be ignored (Eckert and Drake [3]). In view of the importance of this diffusion-thermo effect, Jha and Singh [5] studied the free convection and mass transfer flow about an infinite vertical flat plate moving impulsively in its own plane, taking into account the Soret effects. Kafoussias [6] studied the same problem in the case of MHD flow. They made analytical studies based on the Laplace Transformation technique. Later, Kafoussias and

Corresponding Author: Meenakshi, V, Osmania University, India.
Email: meena123gajender@gmail.com

Williams [7] studied thermal-diffusion and diffusion-thermal effects on mixed free-forced convective and mass transfer boundary layer flow with the temperature dependent viscosity. Whereas Anghel et al. [2] investigated the Dufour and Soret effects on a free convection boundary layer over a vertical surface embedded in a porous medium. Recently, Takhar et al. [18] studied unsteady free convection flow over an infinite porous plate due to the combined effects of thermal and mass diffusion, magnetic field and Hall currents. Postelnicu [10] studied numerically the influence of a magnetic field on heat and mass transfer by natural convection from vertical surface in porous media considering Soret and Dofour effects. The Diffusion-thermo and thermal-diffusion effects on free convective heat and mass transfer flow in a porous medium with time dependent temperature and concentration is studied.

Therefore the objective of this paper is to study the Dufour and Soret effects on unsteady free convection and mass transfer flow, past an impulsively started infinite vertical porous flat plate, of a viscous incompressible and electrically conducting fluid in the presence of a uniform transverse magnetic field by considering permeability parameter.

2. Mathematical Analysis

We consider an unsteady two-dimensional flow of an incompressible and electrically conducting fluid, along an infinite vertical porous flat plate. The x-axis is taken along the plate in the upward direction and the y-axis is taken normal to the plate. A magnetic field of uniform strength is applied transversely to the direction of the flow. Initially the plate and the fluid are at the same temperature $T_\infty >$ in stationary condition with concentration level $C_\infty >$ at all points. For time t>0, the plate starts, moving impulsively in its own plane with a velocity U_∞ its temperature is raised to T_w and the concentration level at the plate is raised to C_w. The fluid is assumed to have constant properties except for the influence of the density variations with temperature and concentration, which are considered only in the body force term. From the work done by and Under the above assumptions, the physical variables are functions of y and t only and therefore the basic equations, which govern the problem, are:

$$\frac{\partial v}{\partial y} = 0 \tag{1}$$

$$\frac{\partial v}{\partial y} + v\frac{\partial u}{\partial y} = \left(v\frac{\partial^2 u}{\partial y^2}\right) + g\beta(T - T_\infty) + g\beta^*(C - C_\infty) - \frac{\sigma {B_0}^2 u}{\rho} - \frac{v}{kc}u \tag{2}$$

$$\frac{\partial T}{\partial t} + v\frac{\partial T}{\partial y} = \alpha\frac{\partial^2 T}{\partial y^2} + \frac{D_m k_T}{c_s c_p}\frac{\partial^2 C}{\partial y^2} + Q(T - T_w) \tag{3}$$

$$\frac{\partial C}{\partial t} + v\frac{\partial C}{\partial y} = D_m\frac{\partial^2 C}{\partial y^2} + \frac{D_m k_T}{T_m}\frac{\partial^2 T}{\partial y^2} \tag{4}$$

where the variables and related section quantities are defined in the Nomenclature section. The initial and boundary conditions for the above problem are:
for $t \le 0: u = v = 0. T = T_\infty C = C_\infty$ for all y

$$\text{for } t > 0: u = U_0. v = v(t). \quad T = T_w. C = C_w \text{ for all } y = 0 \tag{5a}$$

$$u = 0. v = 0. T = T_\infty. C = C_\infty \text{ as } y \to \infty \tag{5b}$$

The last term on the right-hand side of the energy equation (3) and concentration equation (4) signify the Dufour or diffusion-thermo effect and the Soret or thermal-diffusion effect, respectively.

Now in order to obtain a local similarity solution in the time of the problem under consideration, we introduce a time dependent length scale δ as:

$$\delta = \delta(t) \tag{6}$$

In terms of this length scale, a convenient solution of the equation (1) is considered to be in the following form:

$$v = v(t) = -v_0\frac{\nu}{\delta} \tag{7}$$

$$\left\{\begin{aligned} &\eta = \frac{y}{\delta} \\ &u = U_0 f(\eta) \\ &\theta(\eta) = \frac{T - T_\infty}{T_w - T_\infty} \\ &\phi(\eta) = \frac{C - C_\infty}{T_w - T_\infty} \end{aligned}\right\} \tag{8}$$

Then, introducing the relations equations (6)-(8) into the equations (2), (3) and (4), respectively, we then obtain the following ordinary differential equations:

$$f'' + \eta\left(\frac{\delta}{v}\frac{d\delta}{dt}\right)f' + v_0 f' + Gr\theta + Gm\phi - Mf - \lambda f = 0 \tag{9}$$

$$-\eta\left(\frac{\delta}{v}\frac{d\delta}{dt}\right)\theta' + v_0\theta' + \frac{1}{Pr}\theta'' + Dr\,\phi'' + s\theta = 0 \tag{10}$$

$$-\eta\left(\frac{\delta}{v}\frac{d\delta}{dt}\right)\phi' - v_0\phi' + \frac{1}{Sc}\phi'' + Sr\theta'' = 0 \tag{11}$$

Where $P_r = \frac{v}{\alpha}$ is the prandtl number, $Sc = \frac{v}{D_m}$ is the Schmidt number, $M = \frac{\sigma B_0^2 \delta^2}{v\rho}$ is the Magnetic field parameter, $\boldsymbol{s} = \left(\frac{Q}{pCp}\right)$ is the heat Source/Sink parameter, $S_r = \frac{D_m k_T (T_w - T_\infty)}{T_m v (C_w - C_\infty)}$ is the Soret number, $Df = \frac{D_m k_T (C_w - C_\infty)}{c_s c_p v (T_w - T_\infty)}$ is the Dufourt number, $Gr = \frac{g\beta(T_w - T_\infty)\delta^2}{vU_0}$ is the local Grashof number, $Gm = \frac{g\beta^*(C_w - C_\infty)\delta^2}{vU_0}$ is the local modified Grashof number.

The corresponding boundary conditions for t>0 are obtained as:

$$f = 1. \theta = 1. \phi = 1. \text{ at } \eta = 0 \tag{12a}$$

$$f = 0. \theta = 0. \phi = 0. \text{ at } \eta = \infty \tag{12b}$$

Now the equations (9)-(11) are locally similar except the term $\left(\frac{\delta}{\nu}\frac{d\delta}{dt}\right)$, where t appears explicitly. Thus, the local similarity condition requires that the term $\left(\frac{\delta}{\nu}\frac{d\delta}{dt}\right)$ in the equations (9)-(11) must be a constant quantity.

Hence, following the works of Hasimoto [4], Sattar and Hossain [13], and Sattar et al. [14], one can try a class of solutions of the equations (9)-(11) by assuming that:

$$\left(\frac{\delta}{\nu}\frac{d\delta}{dt}\right) = \lambda \qquad (a\ constant) \tag{13}$$

Integrating equation (13) we have:

$$\delta = \sqrt{2\lambda\nu t} \tag{14}$$

Where the constant of integration is determined through the condition that δ=0 when t = 0. We have considered the problem for small time. In this case the normal velocity in equation (7) will be large, which can be applied to increase the lift of airfoils. From equation (14), choosing λ=2, the length scale $\delta(t) = 2\sqrt{\nu t}$ exactly corresponds to the usual scaling factor for various unsteady boundary layer flows (Schlichting [15]). Since δ is a scaling factor as well as a similarity parameter, any value of λ in equation (13) would not change the name of the solutions, except that the scale would be different.

Now introducing equation (13) (with λ=2) in the equations (9)-(11) respectively, we obtain the following dimensionless ordinary differential equations which are locally similar in time but not explicitly time dependent.

$$f'' + (2\eta + \nu_0)f' + \nu_0 f' + Gr\theta + Gm\phi - Mf - \lambda f = 0 \tag{15}$$

$$\theta'' + \Pr(2\eta + \nu_0)\,\theta' + PrDr\Phi'' + Prs\theta = 0 \tag{16}$$

$$\phi'' + Sc(2\eta + \nu_0)\phi' + ScSr\theta'' = 0 \tag{17}$$

Where primes denotes differentiation with respect to η.

Skin-friction, rate of heat and mass transfer:

Now it is important to calculate the physical quantities of the primary interest, which are the local wall shear stress, local surface heat flux and the local surface mass flux respectively from the following definitions:

$$\tau_w = \mu\left(\frac{\partial u}{\partial y}\right)_{y=0} \tag{18}$$

$$q_w = -k\left(\frac{\partial T}{\partial y}\right)_{y=0} \tag{19}$$

$$M_w = -D\left(\frac{\partial C}{\partial y}\right)_{y=0} \tag{20}$$

Where μ is the viscosity, K is the thermal conductivity and D_m is the mass diffusivity.

The dimensionless local wall shear stress, local surface heat flux and the local surface mass flux for an impulsively started plate are respectively obtained by:

$$\frac{\tau_w\delta}{\mu U_0} = f'(0) \tag{21}$$

$$\frac{q_w\delta}{k(T_w - T_\infty)} = -\theta'(0) \tag{22}$$

$$\frac{M_w\delta}{D_m(C_w - C_\infty)} = -\phi'(0) \tag{23}$$

Hence the dimensionless skin-friction coefficient, Nusselt number and Sherwood number for impulsively started plate are given by:

$$C_f = \frac{2\tau_w}{\rho U_0^2} = 2(Re_\delta)^{-1} = f'(0) \tag{24}$$

$$Nu = \frac{q_w\delta}{k(T_w - T_\infty)} = -\theta'(0) \tag{25}$$

$$Sh = \frac{M_w\delta}{D_m(C_w - C_\infty)} = -\phi'(0) \tag{26}$$

$Re_\delta = \frac{U_0\delta}{\nu}$ is the Reynolds number.

These dimensionless values of the local skin-friction coefficient, local Nusselt number and local Sherwood number for impulsively started plate are obtained from the process of numerical calculations and are sorted in Tables 1-3.

3. Method of Solution

The equations (15)-(17) constitute a set of ordinary equations, the solutions of which should unfold the characteristic of the problem under consideration. These equations under the boundary conditions equation (12) are solved numerically by using the Implicit finite difference method. Substituting the finite difference formulae

$$f'(i) = \frac{f(i+1) - f(i-1)}{2h}$$

$$f''(i) = \frac{f(i+1) - 2f(i) + f(i-1)}{h^2}$$

in equations (15)-(17) we get,

$$A_1[i]f[i+1] - A_2 f[i] + A_3[i]f[i-1] + A_4[i] + A_5[i] = 0 \tag{27}$$

$$B_1 * \theta[i+1] - B_2 * \theta[i] + B_3 * \theta[i-1] + B_4[i] * D_1[i] = 0 \tag{28}$$

$$C_1\phi[i+1] - 4*\phi[i] + C_2\phi[i-1] + C_3[i]*D_2[i] = 0 \quad (29)$$

Where

$$A_1[i] = 2 + h*A[i]$$

$$A_2[i] = 4 + 2*h^2*(M+\lambda)$$

$$A_3[i] = 2 - h*A[i]$$

$$A_4[i] = 2*h^2*G_r*\theta[i]$$

$$A_5[i] = 2*h^2*G_m*\phi[i]$$

$$B_1 = 2 + h*Pr$$

$$B_2 = 4 - 2*h*h*Pr*s$$

$$B_3 = 2 - h*Pr$$

$$B_4[i] = 2*h^2*Pr*Df$$

$$C_1 = 2 + h*Sc$$

$$C_2 = 2 - h*Sc$$

$$C_3[i] = 2*h^2*Sc*Sr$$

$$D_1[i] = \frac{\phi[i+1] - 2*\phi[i] + \phi[i-1]}{h^2}$$

$$D_2[i] = \frac{\theta[i+1] - 2*\theta[i] + \theta[i-1]}{h^2}$$

To obtain the numerical solutions the equations (27) - (29) with boundary conditions (12a) & (12b) are solved by using the Gauss-Siedel iterative method. Here h represents the mesh size in η direction. For convergence of a solution of a solution, after each cycle of iteration, the tolerance is set at 10^{-6} is satisfied at all points.

4. Results and Discussion

In order to get a clear insight of the physical problem, numerical results are displayed with the help of graphical illustrations. The velocity profiles, temperature profiles and concentration profiles of the fluid are shown graphically for different flow parameters: suction parameter ν_0, magnetic field parameter M and for the fixed values of Prandtl number *Pr*, Schmidt number *Sc*, Grashof number *Gr* and modified Grashof number *Gm* are represented. The values of *Gr* and *Gm* are taken to be both positive and negative, since these values represents respectively, cooling and heating of the plate. Finally the values of Soret number *Sr*, Dufour number *Df* are chosen in such a way that their product is constant. The value of the Prandtl number *Pr* is taken equal to 0.71 which corresponds physically to air. The value of the Schmidt number *Sc*=0.22 has been chosen to represent the hydrogen at approx T_m = 25ºC and 1 atm.

The velocity profiles for different values of suction parameter ν_0 and magnetic field parameter *M* are shown in fig 1., for both cooling (*Gr,Gm*>0) and heating (*Gr,Gm*<0) of the plate. This figure shows that for cooling of the plate the velocity profiles decreases monotonically with the increase of suction parameter, where as the velocity profiles increases with the increase of ν_0 for heating of the plate. For cooling of the plate and for fixed suction parameter, the velocity profile found to increase and reaches a maximum value in a region close to the surface of the plate, then gradually decreases to zero. It is also observed that as the magnetic field parameter increases the velocity decreases for the cooling of the plate, where as increases for heating of the plate.

The effects of Soret number *Sr* and Dufour number *Df* on the velocity field for cooling and heating of the plate are shown in fig 2. It is noticed that for cooling of the plate, quantitatively when η=0.5 and as *Sr* decreases from 2 to 0.1 (or Dufour number *Df* increases from 0.03 to 0.60) there is decrease in the velocity profiles. The permeability parameter λ effects on the velocity profiles are shown in fig 3 for both cooling and heating of the plate. It is observed that with the increase in λ, the velocity profiles decreases for cooling, while it is increases for heating of the plate. In this figure, when compared to the case of the cooling of the plate, opposite effects are observed in the case of heating the plate. Fig 4 is drawn for the effect of the heat source/ sink parameter 's' on the velocity profiles f(λ). The velocity profiles increases for cooling as well as for heating of the plate with the increase of heat source parameter.

The energy and concentration equations are independent of all parameters except the suction parameter, Dufour and Soret numbers. The dimensionless temperature profiles are drawn for cooling of the plate. From fig 5 it is noticed that the temperature profiles decreases with the increase in suction parameter. The temperature distribution of the fluid increases with increase in Dufour number from 0.03 to 0.60 (or decrease in Soret number from 2.0 to 0.1) is shown in fig 6 when suction parameter ν_0=0.5. The effects of magnetic field parameter *M* on temperature profiles leads to increase in temperature distribution is shown in fig 7.The temperature profiles for different values of heat source/sink parameter 's' is drawn in fig 8. From this figure it is observed that the temperature profiles decreases with the increase of heat source parameter.

In figures 9, 10 & 11, the concentration profiles are drawn for cooling of the plate. It is observed from fig 9, that the concentration of the fluid increases close to the wall as the value of suction parameter increases**.** The dimensionless concentration profiles for different values of Soret and Dufour numbers are depicted in fig 10. It is noticed from this figure that the concentration profiles decreases with the increase in Dufour number or decrease in Soret number. From fig 11 the concentration distribution increases with the increase in magnetic field parameter M is noticed. Fig 12 represents the concentration profiles for different values of heat source/ sink parameter 's'. The concentration profiles increases as heat source parameter increases.

The effects of various parameters on Skin-friction coefficient Cf, Nusselt number Nu and Sherwood number Sh are shown in Tables 1, 2, &3. From table 1 it can be seen that the effect of the magnetic field parameter M on the Skin-friction Cf is increases for heating of the plate, while it reduces for the cooling of the plate. The Skin friction coefficient Cf decreases with the increase of suction parameter ν_0, for the both heating and cooling of the plate.

The Skin-friction coefficient Cf decreases with the decrease of Soret number Sr (or with the increase of the Dufour number Df) for cooling of the plate, where as reverse effect have seen in heating of the plate in Table 2. For the cooling of the plate the Cf decreases as the permeability parameter increases, while opposite effect is observed for heating of the plate in the Table 3.

The Nusselt number Nu value increases with the effect of suction parameter ν_0, while it decreases with the effect of magnetic field parameter M is shown in Table 1. With the decrease of Sr (or increase of Df) the value of Nu decreases, which is depicted in Table 2. It can be seen from Table 3, that no change in Nu and Sh for the different values of permeability parameter λ.

The Sherwood number Sh is decreases as the suction parameter ν_0 increases and magnetic field parameter M increases is shown in Table 1. Whereas Sh increases while decreasing Sr (or increasing Df) can be observed in Table 2.

Table 1. Numerical values of Skin-friction coefficient, Nusselt number and Sherwood number for Pr=0.71, Sr=2.0, Df=0.03, Sc=0.22.

Gr	G_m	M	ν_0	C_f	Nu	Sh
-2	-10	0.2	0.5	-10.224621	1.730404	-0.081845
-2	-10	0.2	1.0	-10.881990	2.936380	-0.45.520
-2	-10	0.2	1.5	-11.511583	4.471137	-1.043057
-2	-10	1.0	1.5	-10.865924	4.365475	-1.043397
-2	-10	3.0	1.5	-9.541916	4.164802	-1.043644
2	10	0.2	0.5	7.206197	1.730404	-0.081845
2	10	0.2	1.0	6.953430	2.936380	-0.450520
2	10	0.2	1.5	6.613309	4.471137	-1.043057
2	10	1.0	1.5	5.488610	4.365475	-1.043397
2	10	3.0	1.5	3.422229	4.164802	-1.043644

Table 2. Numerical values of Skin-friction coefficient, Nusselt number and Sherwood number for Pr=0.71, ν_0=0.5, M=0.2, Sc=0.22.

Gr	G_m	Sr	Df	C_f	Nu	Sh
2	10	2.0	0.03	7.745465	1.9855619	0.087549
2	10	0.4	0.15	5.621989	1.549031	0.492942
2	10	0.4	0.60	5.816160	1.373755	0.573434
-2	-10	2.0	0.03	-10.716802	1.9855619	0.087549
-2	-10	0.4	0.15	-8.397187	1.549031	0.492942
-2	-10	1.0	0.60	-8.050458	1.373755	0.573434

Table 3. Numerical values of Skin-friction coefficient, Nusselt number and Sherwood number for Pr=0.71, Sc=0.22, Sr=2.0, Df=0.03 ν_0=0.5, M=0.2

Gr	G_m	λ	Cf	Nu	Sh
2	10	0.1	7.586002	1.730404	-1.178072
2	10	0.5	6.803537	1.730404	-1.178072
2	10	0.9	6.129960	1.730404	-1.178072
-2	-10	0.1	-11.831.683	1.730404	-1.178072
-2	-10	0.5	-10.914897	1.730404	-1.178072
-2	-10	0.9	-10.145585	1.730404	-1.178072

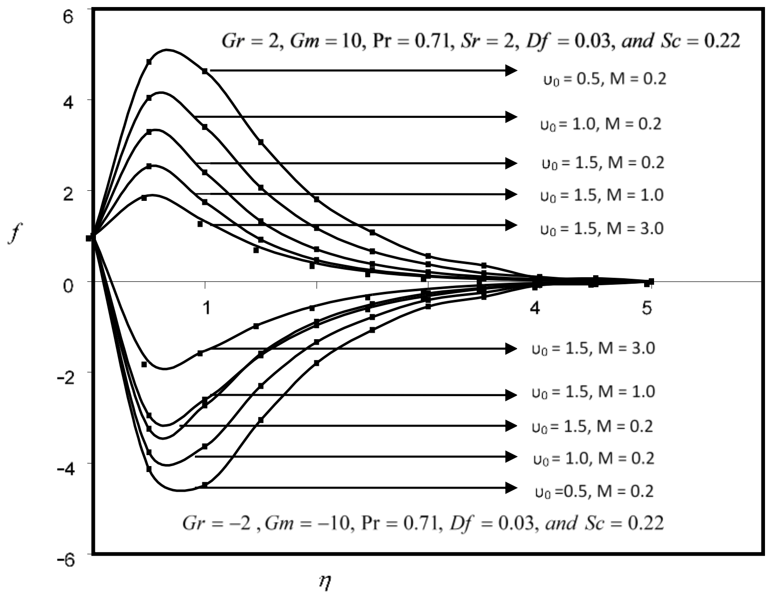

Fig. 1. Velocity profiles for different values of $v_0$and M.

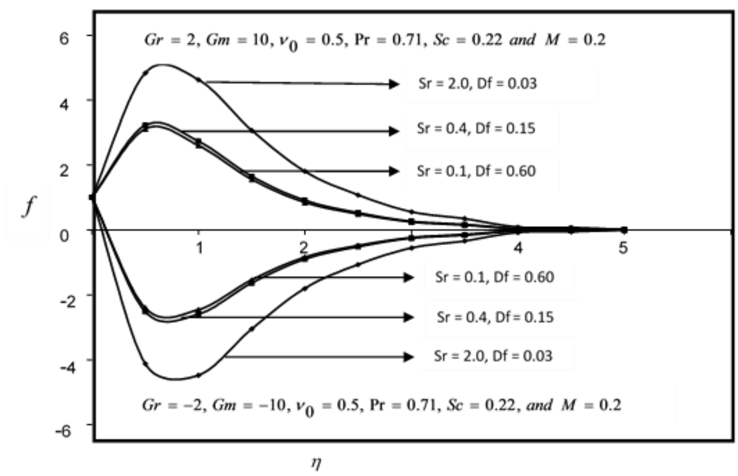

Fig. 2. Velocity profiles for different values of *Sr* and *Df*.

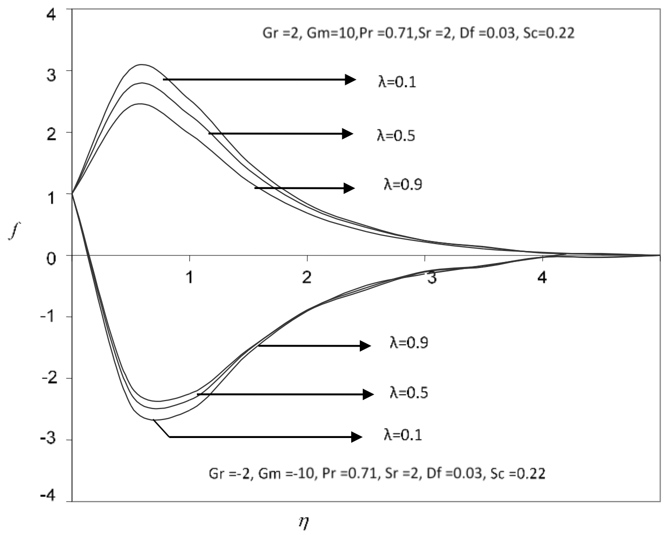

Fig. 3. Velocity profiles for different values of λ.

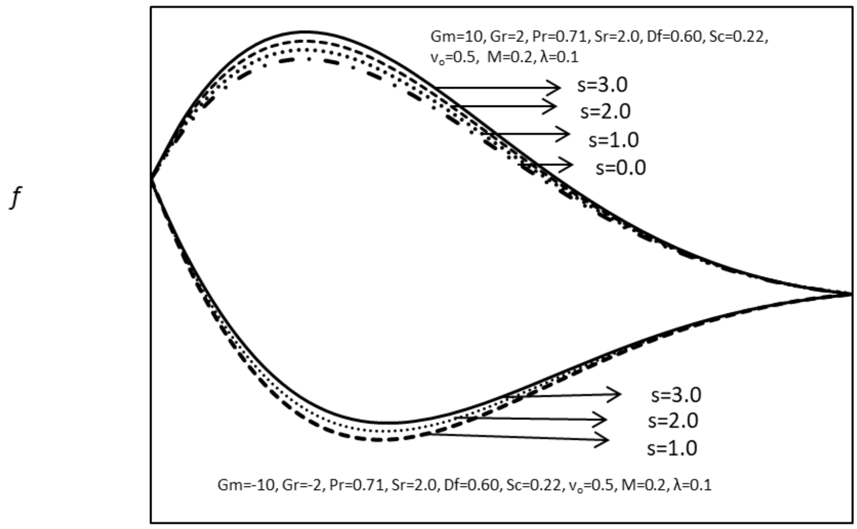

Fig. 4. Velocity profiles for different values of ***s***.

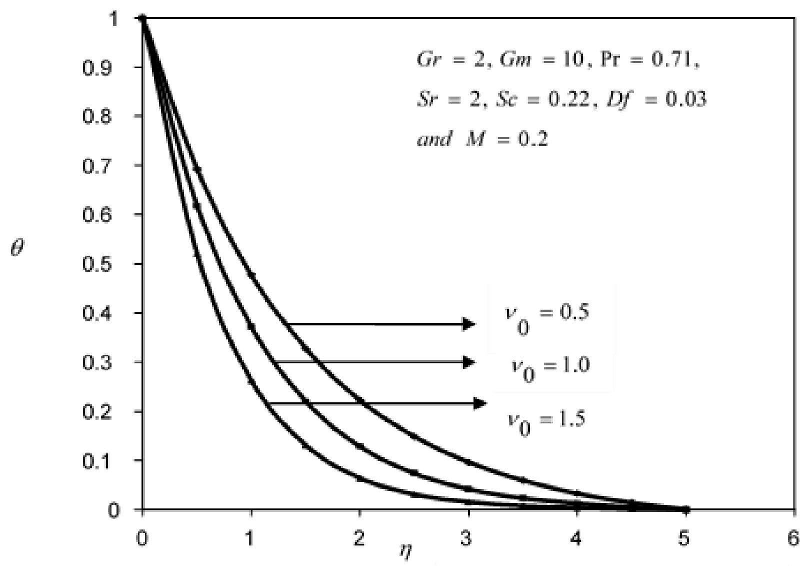

Fig. 5. Temperature profiles for different values of υ_0

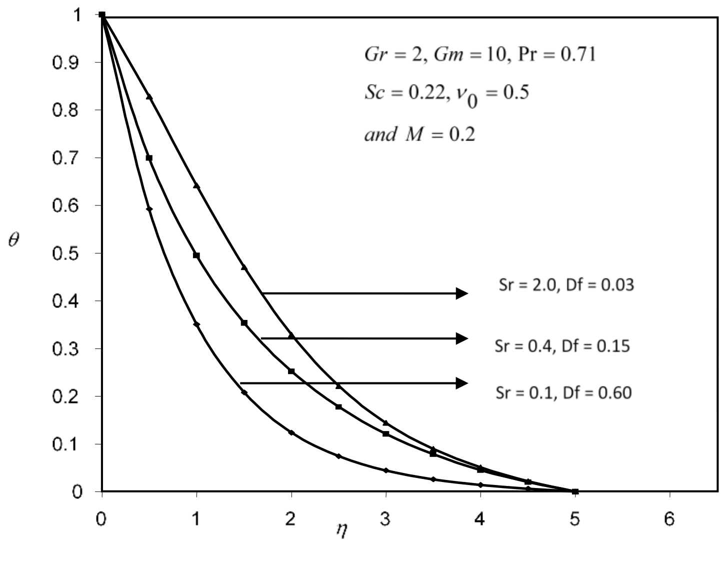

Fig. 6. Temperature profiles for different values of *Sr*

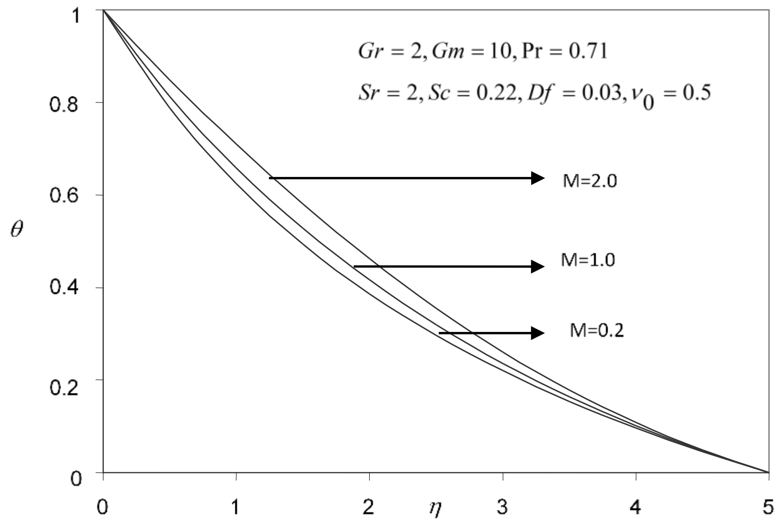

Fig. 7. Temperature profiles for different values of M.

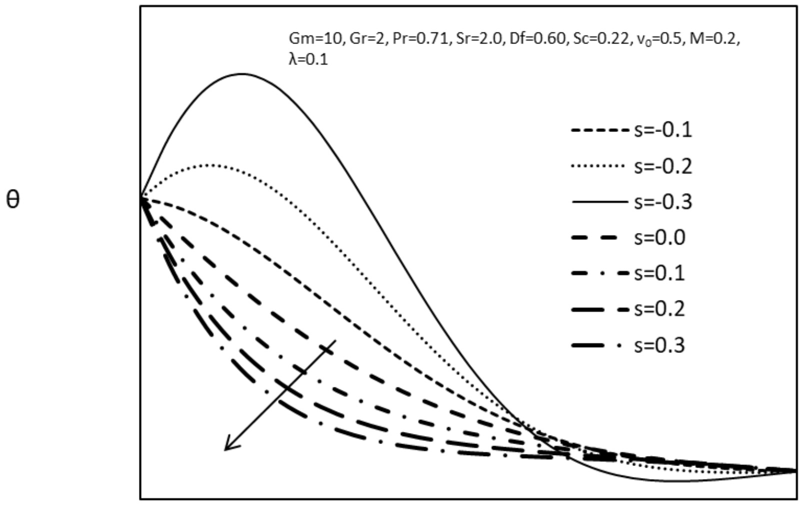

Fig. 8. Temperature profiles for positive and negative values of ***s***.

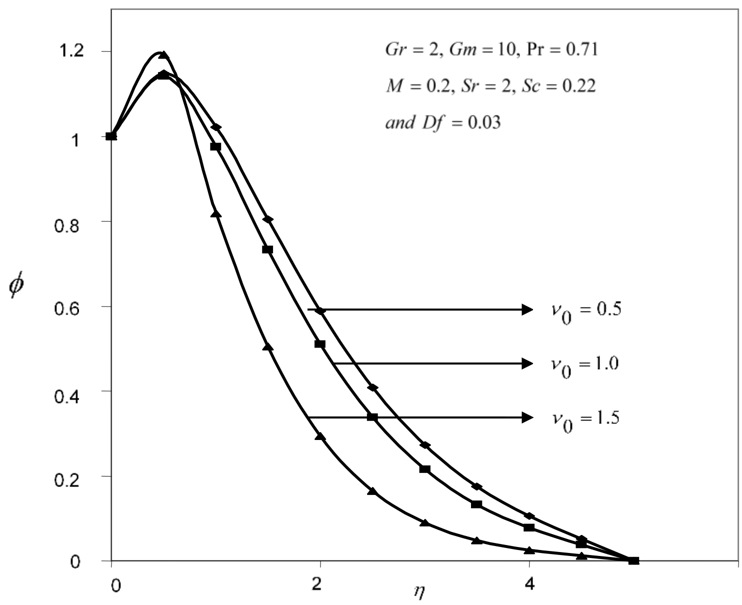

Fig. 9. Concentration profiles for different values of υ_0

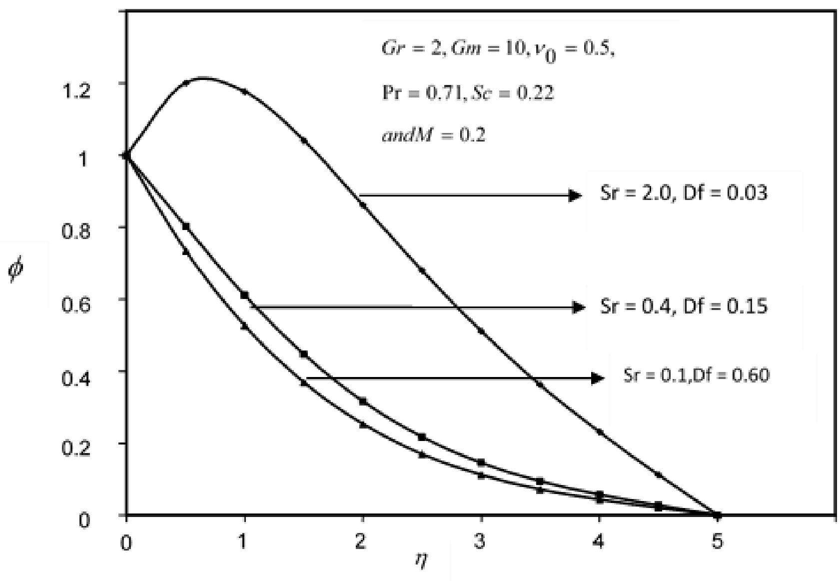

Fig. 10. Concentration profiles for different values of Sr and Df.

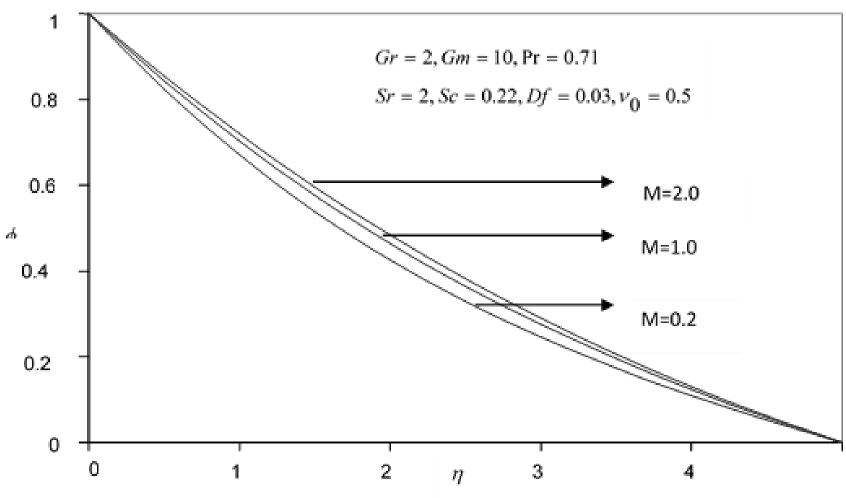

Fig. 11. Concentration profiles for different values of *M*.

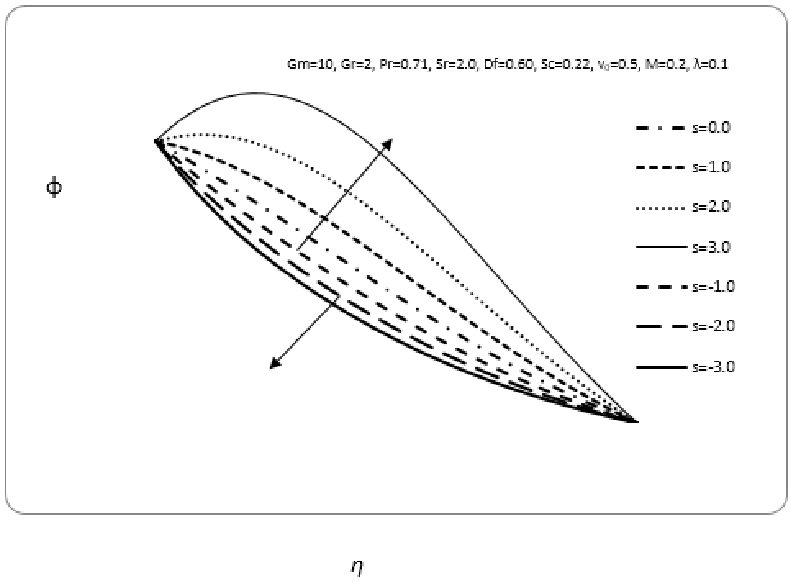

Fig. 12. Concentration profiles for positive and negative values of ***s***.

References

[1] Aboeldahab, E. M. and Elbarbary, E. M. E., 2001, 'Hall current effect on Magneto hydrodynamic Free Convection Flow Past A Semi-Infinite vertical Plate with Mass Transfer' *INT. J. ENGNG. SCI.*, vol. 39, pp.1641-165

[2] Anghel, M., Takhar, H. S. and Pop. I, 2000, 'Dufour and Soret effects on Free Convection Boundary layer Over a Vertical Surface Embedded in a Porous Medium', *STUDIA UNIVERSITATIS BABES-BOLYAI, MATHEMATICA,* vol. XLV, pp. 11-21.

[3] Eckert, E. R. G. and Drake, R. M., 1972, 'Analysis of Heat and Mass Transfer', *MCGRAW-HILL, NEW YORK*.

[4] Hasimoto, H. 1956, 'Boundary Layer Growth on a Flat plate with Suction or injection', *J. PHYS. SOC. JAPAN.*, vol. 12, pp.68-72.

[5] Jha, B. K. and Singh, A. K. 1990, 'Soret Effects on Free Convection and Mass transfer flow in the Stokes Problem for an Infinite vertical plate' *ASTROPHYS. SPACE SCI.,* vol. 173, pp.251-255.

[6] Kafoussias, N. G.,1992, 'MHD Thermal-Diffusion Effects on Free convective and Mass Transfer Flow over an infinite vertical moving plate', *ASTROPHYS. SPACE SCI.*, vol.192, pp.11-19.

[7] Kafoussias, N. G. and Williams, E. W., 1995, 'Thermal-diffusion and Diffusion-thermo Effects on Mixed free forced convective and Mass Transfer boundary layer flow with the temperature dependent viscosity', *INT. J. ENGNG. SCI.*, vol. 33, pp.1369-1384.

[8] Kim, Y. J. 2004, 'Heat and Mass Transfer in MHD Micro polar flow over a vertical moving porous medium', *TRANSPORT IN POROUS MEDIA*, vol. 56, pp.17-37.

[9] Megahead, A. A., KOMY, S. R. and Afify, A. A., 2003, 'Similarity Analysis in Magneto hydrodynamics Hall Effects on Free convection flow and Mass Transfer past a Semi-Infinite vertical flat plate', *INER. JOUR. NON-LINEAR MECHA.,* vol. 38, pp.513-520.

[10] Postelnicu, A., 2004, 'Influence of a Magnetic field on Heat and Mass transfer by Natural Convection from vertical surfaces in porous media considering Soret and Dufour Effects', *INT. J. HEAT MASS TRANSFER*, vol. 47, pp.1467-1472.

[11] Rahman, M. M. and Sattar, M. A.,1999, 'MHD free convective and Mass transfer flow with Oscillatory plate velocity and constant Heat source in a rotating frame of reference', *DHAKA UNIV. J. SCI.*, vol. 49(1), pp.63-73.

[12] Raptis, A. and Kafoussias, N.G.,1982, 'Magneto hydrodynamics free convection flow and Mass transfer through porous medium bounded by an infinite vertical porous plate with constant Heat flux', *CAN. J. PHYS.*, vol. 60, pp.1725-1729.

[13] Sattar, M. A. and Hossain, M. M., 1992, 'Unsteady Hydro magnetic free convection flow with Hall Current and Mass transfer along an accelerated porous plate with time dependent temperature and concentration', *CAN. J. PHYS.,* vol. 70, pp.68-72.

[14] Sattar, M. A., Rahman, M. M. and Alam, M. M., 2000, 'Free convection flow and Heat Transfer through a porous vertical flat plate immersed in a porous medium with variable suction', *J. ENERGY HEAT AND MASS TRANSFER*, vol. 22, pp. 17-21.

[15] Schlichting, H., 1968, 'Boundary Layer Theory', 6th Edition, *MCGRAW-HILL, NEW YORK.*

[16] Soundalgekar, V. M. 1977, 'Free convection effects on the Stokes Problem for an infinite vertical plate, ASME J. Heat Transfer', vol. 99, pp.499-501.

[17] Stokes, G. G., 1856, 'On the Effects of the Internal Friction of fluids on the motion of pendulum', *TRANS. COMBR. PHIL. SOC.*, vol.9, pp.8-106.

[18] Takhar, H. S., Roy, S. and Nath, G., 2003, 'Unsteady Free convection flow over an infinite porous plate due to the combined effects of thermal and mass diffusion, magnetic field and Hall Currents', *HEAT AND MASS TRANSFER*, vol. 39, pp.825-834.

[19] Yih, K. A., 1999, 'Free convection effect on MHD coupled Heat and Mass transfer of a moving permeable vertical surface', *INT. COMM. HEAT MASS TRANSFER,* vol. 26, pp. 95-104.